Submitted to ApJL

# On the Ordinary Characteristics of the Medium Responsible for the Extreme Scattering Events

Avinash A. Deshpande[1]

*NAIC/Arecibo Observatory, HC3 Box 53995, Arecibo, Puerto Rico 00612*

desh@naic.edu

and

V. Radhakrishnan

*Raman Research Institute, C. V. Raman Avenue, Bangalore 560 080 INDIA*

rad@rri.res.in

## ABSTRACT

Extensive monitoring of compact extra-galactic radio sources over the last few decades has revealed many instances of intensity variations of unusual magnitude and duration, termed Extreme Scattering Events. Many models invoking refractive effects due to localized/discrete structures in the ionized component of the ISM have been proposed to explain the observations. These models, however, imply electron density enhancements (as well as pressures) that are 2 to 3 orders of magnitude higher than indicated by other probes.

It is quite possible that the observed effects are not due to any mysterious discrete concentrations, but rather just the combined manifestation of fluctuations on a whole range of hierarchical scales in the distribution of the ionized matter. In this paper, we argue that a single power-law description of the electron density distribution in the ISM is consistent with the observations. We also examine the assumptions leading to the earlier estimates of the implied enhancements in the electron density (and pressure) and find no compelling evidence for such over-dense structures. Details of our simulations and results are presented.

[1]Raman Research Institute, C. V. Raman Avenue, Bangalore 560 080 INDIA; e-mail:desh@rri.res.in

*Subject headings:* Plasmas — Scattering — Turbulence — Methods: numerical — ISM: general, structure, kinematics and dynamics — Radio continuum: general — Galaxies: ISM

## 1. Introduction

In an extensive study of a large number of compact extra-galactic radio sources at 2.7 GHz & 8.1 GHz over more than a decade, Fiedler et al. (1987,1994) have detected intensity variations of unusual magnitude and duration. They argued that such variations are unlikely to be intrinsic to the source, and suggested that refractive effects in the interstellar medium are probably responsible. So far, 10 such unusual variations, termed Extreme Scattering Events, have been tentatively identified in the 2.7 GHz light curves of nine quasars. A significant variety is seen in the event shapes at 2.7 GHz, and interestingly, most events have no counterpart at 8.1 GHz (Fiedler et al. 1994).

Several models invoking refractive effects due to localized/discrete (AU-scale) structures in the ionized component of the ISM have been proposed to explain the observations (Romani, Blandford & Cordes 1987; Romani 1988; Fiedler et al. 1994; Clegg, Fey & Lazio 1998; Walker & Wardle 1998). In these models, the observed magnitude and the duration of the intensity variations relate primarily to the parameters (associated column density & transverse scale size) of the discrete structure responsible. Clegg, Fey & Lazio (1998) have analyzed in detail the case of Gaussian plasma lenses and argue for 'weak' plasma lenses to explain the general lack of caustic spikes in ESEs. These models, however, imply electron density enhancements (as well as pressures) that are invariably 2 to 3 orders of magnitude higher than indicated by other probes, such as diffractive and refractive scintillations of pulsar signals. Naturally, there are serious difficulties about such a structure being in pressure equilibrium with the other components of the medium given the high estimated volume density; also as to what processes could generate and help maintain such discrete structures. Less extreme densities would be implied if such structures were to be *highly* elongated *and* also aligned along the sight-line (e.g. Romani et al 1987). While the model light-curves agree well with those observed at 2.7 GHz, their simultaneous match with the observed behaviour at 8.1 GHz in most cases is rather poor.

One of the important questions raised by the inferred density variations on the sub-AU (spatial) scales, and not often asked, is the following. Is it likely that the observed

effects are not due to any mysterious discrete concentrations, but rather just the combined manifestation of a whole range of hierarchical scales constituting the distribution of the ionized medium ? In this paper, we examine this possibility in detail and assess whether a single power-law description of the ionized component (available from other probes) is consistent with the ESE observations. We also examine the assumptions leading to the earlier estimates of the implied enhancements in the electron density (& pressure).

## 2. Essential characteristics of the medium implied by ESEs: Are they really surprising ?

It is important to note the essential features of the refractive medium relevant to ESEs. The recent characterization and the modelling involving Gaussian plasma lenses by Clegg, Fey & Lazio (1998) provides ready input in this regard. Although our basic premise differs from theirs, the estimates of the column density and scale sizes of the refractors are of common relevance. They estimate column density contrasts of about 0.2 pc $cm^{-3}$ and 0.004 pc $cm^{-3}$ associated with lenses of size 0.4 AU and 0.07 AU respectively in two cases discussed in detail. These estimates are sensitive to certain assumptions (particularly about the scatterer distance) and are based on 1-dimensional modelling. The latter aspect would over-estimate the column-density contrast by a factor of 2 or more. While keeping this in mind, we will treat them as adequately indicative for the present query.

If these parameters are attributed to "single" lenses, then the reported ultra-high plasma density estimates are unavoidable even if appropriate allowance is made for possible elongated shapes. The qualitative parallel between this situation and that of the so-called small-scale ($\sim$10AU-scale) structure in HI is too striking to be ignored, and in our opinion, not a mere coincidence. With regard to the latter, it has been shown recently (Deshpande 2000) that the HI opacity variations observed over transverse scales of tens to hundreds of AU do not necessarily suggest "cloudlets" of comparable scale-size. In fact, the observed variations are only to be expected from a combined manifestation of a whole range of hierarchical scales following a single power-law distribution. More importantly, the implied number densities of HI then turn out to be consistent with those indicated by the pc-scale structures and pressure equilibrium.

To be able to assess the parallel further, we need a description of the electron density distribution in the ISM. In this connection, we refer to the work of Armstrong, Rickett & Spangler (1995) and Bhat, Gupta & Rao (1999), where a composite electron-density spectrum has been estimated based on observations probing diffractive/refractive effects in the ISM. The spectral estimates span over 5 or more orders of magnitudes in spatial scales. Bhat et al. (1999) also give useful estimates of the densities associated with the

large-scale (∼10 AU) features they probe through scintillation drift-bands observed for some pulsars. Their data indicate noticeably increased power at these large scales compared to that expected from smaller scales using a Kolmogorov power-law. Also, interestingly, the estimated densities are of only a few electrons per $cm^3$. Using these spectral descriptions, we examine the structure function of the column-density contrast (or dispersion measure variation) expected on a range of scales, as given in Figure 1. The scale associated with the column-density contrast along the vertical axis is calibrated such that the maximum spatial scale on the horizontal axis would correspond to 100 AU, and is determined based on the comprehensive description of the phase structure function given by Armstrong et al. (1995; their Figure 2), after scaling their results for a 3kpc pathlength. It is easy to see from this structure function equivalent description that the column density variations over the sub-AU scales that *could* result in ESE are not at all unexpected, although the necessary 2-d focusing or defocusing situations may still be relatively rare.

We would like to emphasis that all transverse scales (i.e. spatial frequencies) contribute to the resultant column density profiles in a 2-d distribution in addition to the implicit integration along the longitudinal direction. Therefore, the column density contrast on small scales (e.g. sub-AU scale) should not be interpreted as due to a discrete structure of comparable scale in 3-dimensions. When interpreted correctly, the column density variations implied by ESEs would imply only moderate values of electron (number) density consistent with equilibrium conditions over a range of hierarchical scales. The exact quantitative estimates would depend on the details of the spectrum over the relevant spatial-scales.

We now turn to the important differences in the two (ESE & HI small-scale) situations. The directly observed quantity in the ESE case is the intensity variation due to focusing and defocusing of rays by the (density, and hence, phase) curvatures introduced at the scatterer location. Given a column density contrast, the lensing would be more effective when it is truly 2-dimensional. This naturally makes the strong lensing statistically less probable, qualitatively consistent with the observed frequency of ESEs. The exact nature of the intensity distribution in the observer's plane depends on the detailed geometrical optics (combining the effect of all refractive scales) as well as on the diffractive contributions and the effect of the source size. Any further assessment of our model of the ESE scatterers would need to incorporate these details. We describe in the following section our attempts[1] to do this using Monte Carlo simulations.

---

[1]The preliminary results were reported at the IAU Colloquium 182 in on "Sources and Scintillations: Refraction and Scattering in Radio Astronomy", held at Guiyang, China during 2000.

## 3. Simulations details

For the present investigation, we adopt the approximate model for refractive fluctuations in intensity used by Romani, Narayan & Blandford (1986; hereafter RNB). In their model, the effect of refractive fluctuations in the ISM are treated as perturbations of an underlying bundle of rays scatter-broadened by the diffractive scale inhomogeneities. When averaged over a much longer time scale than that of the diffractive scintillation, the image of a point source is shown to be essentially Gaussian with a characteristic angular radius $\theta$. The Gaussian bundle will be focused, defocused, and tilted by density fluctuations on the scale of the "spot" or image size, $\sigma = \theta L$, where $L$ is the distance of the scattering screen from the observer. Thus, in this model the intensity received at a general point $x$ from unit area around $x+r$ on the scattering screen is weighted proportional to $exp\{-[(L\eta+r)/\sigma]^2\}$, where $\eta$ is the extra refractive bending angle of a ray at transverse locations $(x+r)$ on the screen. Our simulations involve the following steps. More details on these are given in Deshpande & Nityananda (1990).

i) A power-law spectrum for the electron density perturbations is assumed (defined by $Q(q) = Q_0 q^{-\beta}$, with a chosen $\beta$ value). A Hermitian symmetric spectrum, following this average power-law description and with random phases for the contributions at each wave vector ($\bar{q} = (q_x, q_y)$), is simulated in the range $0 < |\bar{q}| \leq q_{ref}$. The cutoff at $q_{ref}$ excludes the short spatial scales which are already accounted for in diffraction broadening of the image. A Fourier transform of this spectrum gives a 2-d distribution of the electron density. The magnitudes can be adjusted to obtain a desired representation in terms of column densities. This calibration step is not crucial, if the magnitudes of the bending angles is calibrated, as described in item-iii below.

ii) From the above, Hermitian symmetric spectra for the bending angles, $\bar{\eta} = (\eta_x, \eta_y)$, are generated from the spectrum of column density distribution by scaling separately with the respective spatial frequencies (i.e. multiplication by -j$q_x$ or -j$q_y$, for $\eta_x$ or $\eta_y$, respectively, where j $= \sqrt{-1}$), and by taking into account the wavelength of observation ($\lambda$). These spectra are Fourier transformed separately to obtain the two components of the extra refractive bending angles ($\bar{\eta}$) at the screen.

iii) The magnitude of $\bar{\eta}$ (w.r.t. $\sigma$) is adjusted, so as to satisfy the relation derived by RNB (their eq. 5.3) between the structure function of $\bar{\eta}$ and the parameter $\sigma$. For simplicity, in our simulations we assume $L = \lambda = C_{-4} = 1$, where $C_{-4}$ is the turbulence level as defined by RNB, and $L$ and $\lambda$ are in kpc and meters respectively. The magnitude of the bending angles depends on a combination of these three parameters.

iv) In order to reduce the number of computations, we adopt the procedure used by

Deshpande & Nityananda (1990). We first find the intensity that would have been observed (following the bending angle distribution), if the diffraction broadening of the image and smoothing due to finite source-size were neglected. This intensity distribution is then convolved with a Gaussian representing the combined effect of the diffractive broadening and the finite intrinsic source size. This procedure gives the same result as would be obtained following integration over $r$.

The simulated intensity patterns, for different assumed values of $\beta$, $\sigma$, and the Fresnel scale, were examined for variations similar to ESEs. In all cases, the 2-d spectra and the corresponding spatial distributions were sampled across a 2048 x 2048 matrix, with its side in the latter case spanning about 30 AU. We assume a nominal transverse speed of 30 km/s for the pattern w.r.t. the observer, making the simulated span equivalent to to about 2000 days in time. Each simulation run, starting with a new realization of the column density spectrum, followed the above described procedure to obtain two separate intensity patterns corresponding to two radio wavelengths ($\lambda$ and $\lambda/2$), but resulting from the same scattering screen. The wavelength dependence of the $\sigma$ and the Fresnel scale was appropriately accounted for.

Results from many hundreds of such runs were subjected to an automated search for the "ESE"s. A simple criterion for selecting 1-d light curves (of 2048 samples each) was employed wherein the most significant "dip" is required to show at least 2:1 contrast with the third most significant feature in that scan. This allowed for the possibility that some scans may have two "ESE"s, and using a relative threshold helped in detecting also the weak but significant "ESE"s. A large number of individual scans passing (or failing) this test were re-examined to verify that the automated procedure had only a small percentage of misses and false alarms. Based on these statistics, we estimate the ESE frequency to be about 1 per 100 source-years. This may appear lower than the frequency of 0.017 events per source-year estimated by Fiedler et al. (1994) based on the 10 ESEs observed in the 594 source-years of monitoring. However, noting the general statistical uncertainty and that the pattern speeds in reality can be significantly higher than our assumed nominal value of 30 km/s, we consider the frequency of ESEs apparent from our simulations to be consistent with that observed. We have examined the results as 1-d light curves sampled along rows or columns of the matrix. In reality, an observer's sampling of the pattern would, in general, be not along a straight line and not with a fixed speed. This aspect may alter the apparent duration of an ESE on a case by case basis, but the apparent frequency of ESE is unlikely to be affected by these details of sampling.

Here, we present a typical sample of an ESE-like intensity variation seen in our simulations (see Fig. 2) for $\beta$ of 11/3. The top and the bottom light curves correspond to

simultaneous measurements simulated at radio wavelengths $\lambda$ and $\lambda/2$, respectively. Events with durations that are a factor of few wider than seen in this example are not very uncommon. There is a mild anticorrelation, on the average, between the depth and the duration of the events apparent in the simulated patterns. The depth of variations depends on the refractive power associated with respective features in the column density distribution as expected. Deeper ESE features result when the overall magnitude of the bending angles is increased. The results obtained with $\beta$ of 4.3 have similar qualitative behaviour as for $\beta$ = 11/3, although caustics appear more readily when the refractive power is increased, as would be expected. More importantly, the frequency of ESEs does not appear to show any significant sensitivity to the value of $\beta$.

## 4. Discussion

In this paper we have addressed some aspects related to the characteristics of the medium responsible for the observed ESEs, in particular, and the column density contrast to be expected on different spatial scales (on the basis of a simple power-law description for the ionized component of the ISM), in general. We have proposed a simple alternative picture in which the essential characteristics implied by ESEs are naturally obtained. Our simulations designed for a more realistic assessment have shown encouraging results in terms of the intensity variations similar to those observed. There seems to be no compelling evidence for the existence of discrete, over-dense, sub-AU scale scatterers that have been proposed so far. A single power-law description of the refractive ionized medium appears consistent with the measurements in the directions of pulsars & compact extra-galactic sources, including ESEs. In general, while estimating number densities from column density variations on some transverse scale, the possible contributions from a) a range of transverse scales (small and long) and b) longitudinal integration should be carefully accounted for. There appears to be no particular need to invoke highly elongated structures in the electron density distribution. Moderate elongations may be implicit, and may only help in lowering the implied number densities.

A detailed quantitative comparison of our model with observations will need some other independent measurements (at least for calibration of the average strength of scattering) in the directions of the ESE sources. A characterization of the ESEs on the lines of Clegg, Fey & Lazio (1998), but with a 2-dimensional modelling, will also be important for a more meaningful comparison.

We would like to thank Rajaram Nityananda and Carl Heiles for their comments on a preliminary version of the manuscript.

## REFERENCES

Armstrong, J. W., Rickett, B. J., & Spangler, S. R. 1995, ApJ, 443, 209

Bhat, N. D. R., Gupta, Y., & Rao, A. P. 1999, ApJ, 514, 249

Clegg, A. W., Fey, A. L., & Lazio, T. J. W. 1998, ApJ, 496, 253

Deshpande, A. A., & Nityananda, R. 1990, A&A, 231, 199

Deshpande, A. A. 2000, MNRAS, 317, 199

Fiedler, R. L., Dennison, B., Johnston, K. J., & Hewish, A. 1987, Nature, 326, 675

Fiedler, R. L., Dennison, B., Johnston, K. J., Waltman, E. B., & Simon, R. S. 1994, ApJ, 430, 581

Romani, R. W., Narayan, R., & Blandford, R. D. 1986, MNRAS, 220, 19

Romani, R. W., Blandford, R. D., & Cordes, J. M. 1987, Nature, 328, 324

Romani, R. W. 1988, in Radio Wave Scattering in the Interstellar Medium, ed. J. M. Cordes, B. J. Rickett, & D. C. Backer (New York: AIP), 156

Walker, M., & Wardle, M. 1998, ApJ, 498, L125

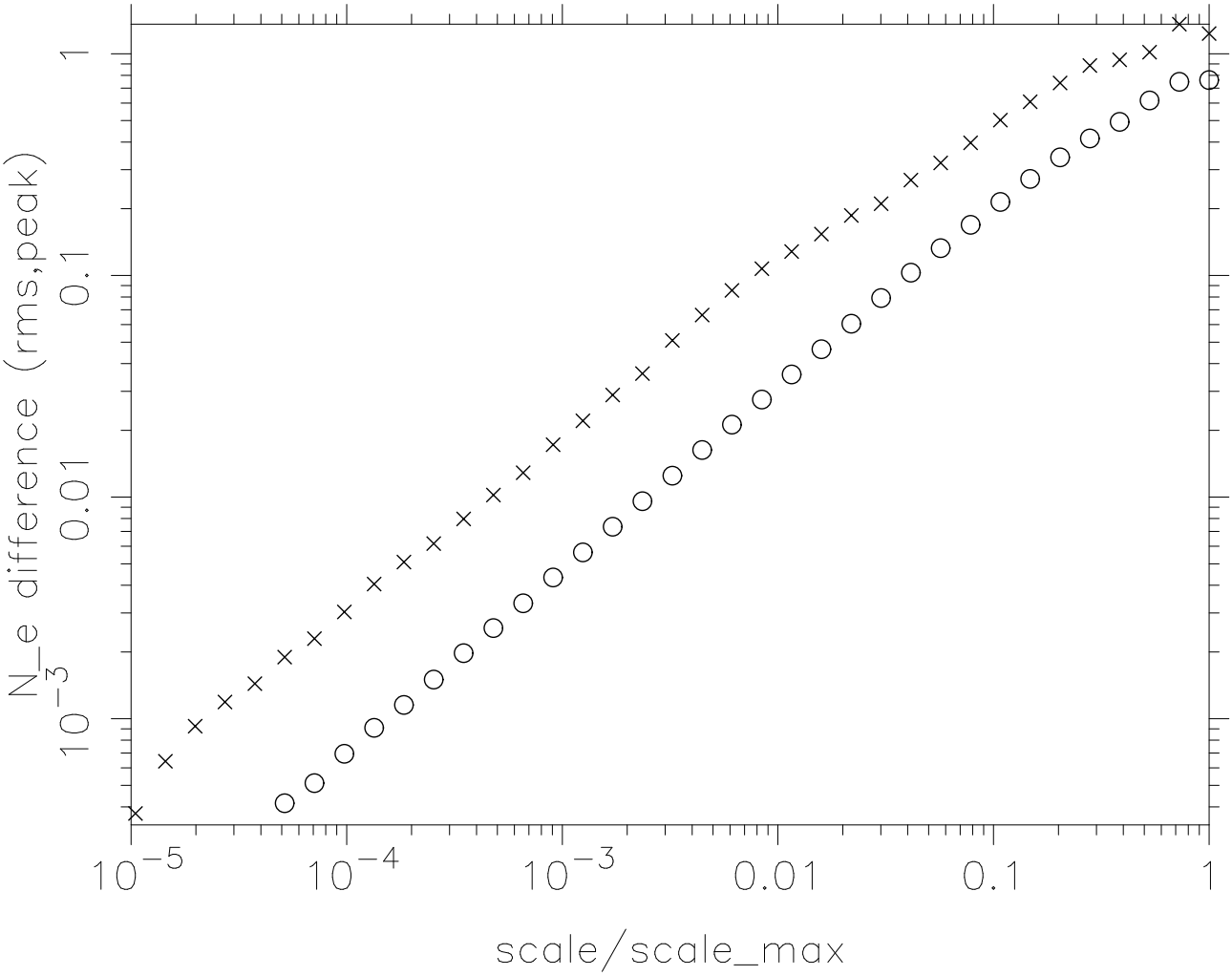


Fig. 1.— Two quantities (related to the magnitude of column density contrast expected as a function of the transverse scale probed) estimated from 1-d simulations of column density distribution are shown. The trends with symbols o,x indicate respectively the rms (i.e. square-root of the structure function) and the typical peak difference magnitudes. The 1-d distribution of column density over 5 orders of magnitude in scales (1:$2^{18}$) was obtained from a simulated spectrum in 1-d with a power-law index $\beta$ of 2.66 (corresponding to a 2-d equivalent index of 11/3). Due to the computational requirements being too high, the 2-d case was not attempted on the same scale-range. The Y-axis values here are calibrated (in units of pc cm$^{-3}$) such that the maximum scale (at the right) may be equated to 100 AU (see text for details). This description provides a ready comparison also for the dispersion measure (DM) variations to be expected on different spatial scales probed by the measurement spans.

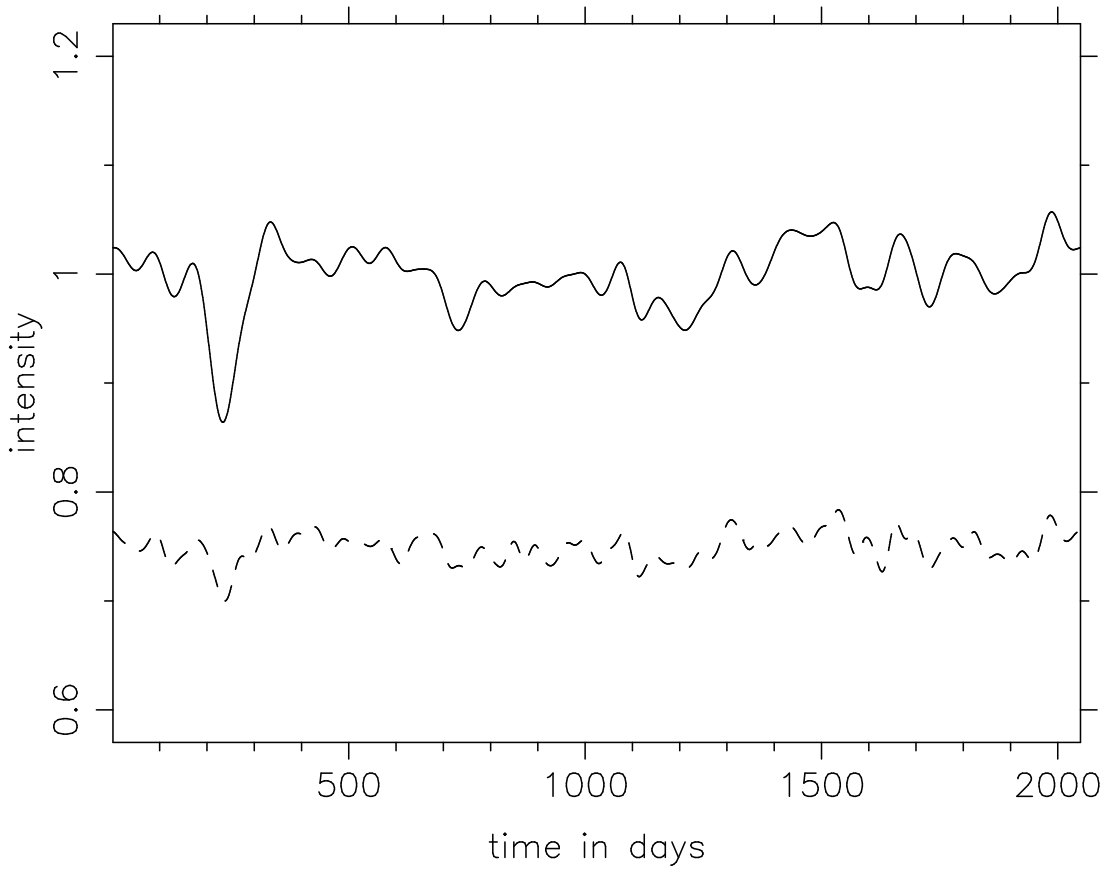


Fig. 2.— A cut through the location of minimum intensity seen in typical (2-d) simulation runs, giving the intensity distribution in the observer's plane, is shown. The span shown corresponds to about 30 AU in spatial scale, and time tags assume a nominal speed of about 30 km/s for the observer w.r.t. the intensity pattern. The top and the bottom light curves depict simultaneous measurements at radio wavelengths $\lambda$ and $\lambda/2$, respectively, with the latter shifted downward by 0.25 for clarity.